Transactions, SMiRT-24
BEXCO, Busan, Korea - August 20-25, 2017
Division V, Paper 408

AUTOMATIC COMPUTATION OF THE STRAIN-DEPENDENT CONCRETE CRACKING PATTERN FOR NUCLEAR STRUCTURES FOR SITE-SPECIFIC APPLICATIONS

Dan M. Ghiocel[1], Mike Saremi[2]

[1] Chief of Engineering and President, Ghiocel Predictive Technologies, Inc., New York, USA
[2] Principal Consultant and Seismic Technical Lead, AMEC Foster Wheeler, Knutsford, UK

INTRODUCTION

The paper presents an efficient nonlinear SSI approach for evaluating the concrete cracking pattern in the nuclear concrete structures. The nonlinear SSI approach is based on a hybrid approach that uses iterative equivalent-linearization models for the concrete wall partitions (panels) that correspond to the local stress/strain levels in different parts of the structure. The local linearized hysteretic wall panel models are calibrated at each SSI iteration based on the "true" nonlinear wall behaviour in the time domain. Refined shear deformation hysteretic models were implemented for low-rise shearwall building applications. Comparative results of the hybrid approach and the *true* nonlinear time-integration approach exhibited very good correlation (Ghiocel, 2015). The hybrid approach is both accurate and extremely fast since convergence is achieved in only few iterations.

This hybrid approach was implemented in the ACS SASSI Option NON software (2016). The nonlinear SSI analysis is applicable to:

i) *Site-specific design level* for accurate evaluation of the concrete cracking pattern in structures as a function of stress/strain levels in accordance with the new ASCE 04-16 standard (Section C3.3.2) and the USNRC SRP requirements for the site-specific license applications, and
ii) *Beyond design level* for structural fragility analyses in accordance with the ASCE 4-16 standard recommendations for using probabilistic nonlinear SSI analysis (Sections 3 and 5.5).

This paper focuses on the evaluation of the concrete cracking pattern in the structure at the design-level for site-specific applications.

EFFICIENT GENERATION OF NONLINEAR STRUCTURAL MODEL

To generate the nonlinear SSI model, the structural walls are subdivided in a number of "panels" for which the assumption of the uniform shear or bending deformation is applicable as shown in Figure 1. Figure 1 shows the external view of the nonlinear structure model split in 40 wall panels (with no roof, basemat and longitudinal external wall. This model split in "panels" can be done by the analyst when the FE model is generated, but also later, using the powerful set of automatic ACS SASSI user-interface (UI) commands. The most important UI commands for building nonlinear models is the PANELGEN command that splits the entire structure or a part of the structure in separate wall panels based on the wall-floor plane intersections. The PANELGEN command maintains the wall height/length aspect ratios above 1/3 to be consistent with the existing experimental test databases for the reinforced concrete (RC) walls. Other specialized commands help analysts to merge or remove wall panels, commands such as the EDGE or EDGEMODEL commands automatically split the wall into separate pier and spandrel panels around the large openings (Figure 2). Thus, generating the nonlinear model is a rapid user-friendly process to build the FE models of nuclear buildings with plane vertical walls and horizontal floors. The UNIPL command is capable of handling curved concrete walls such as the containment shells of the reactor buildings which need to be split at the element level.

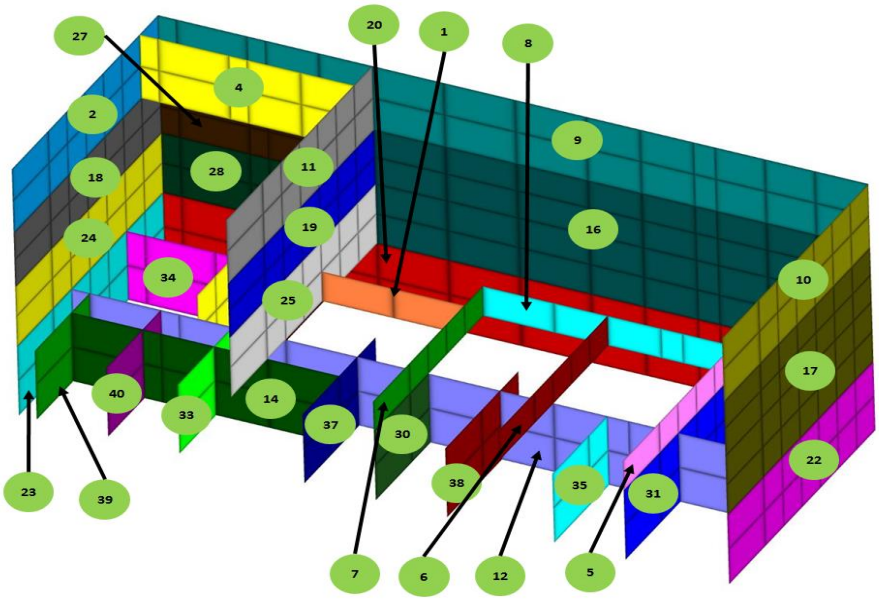

Figure 1 Nonlinear Structure Model Split in Wall Panels

After splitting the nonlinear model into wall panels, the nonlinear behaviour of each panel has to be defined by its back-bone curve (BBC) and hysteretic type model. Three types of nonlinear hysteretic models are available in ACS SASSI Option NON:

i) Cheng-Mertz shear (CMS) model,
ii) Cheng-Mertz bending (CMB) model, and
iii) Takeda model (TAK).

The Cheng-Mertz hysteretic model (Cheng and Mertz, 1989) was used over many years in a number of studies for the DOE and ASCE standards.

It should be noted that the CMS hysteretic model in contrast to TAK model has the capability to better capture the significant shear stiffness degradation for the loading cycle paths for larger seismic loads (similar to an origin-oriented hysteretic model), but also to include the reduced stiffness degradation for the unloading cycle paths and the pinching effects for low amplitude levels as shown in Figure 3. Figure 3 shows the CMS hysteretic loops for a fully converged SSI solution for two random strain histories with the maximum amplitudes of 0.065% that corresponds to the design-basis level DBE input (green line) and, respectively, 0.37% that corresponds to the beyond design-basis level BDBE input that is twice DBE input (red line).

Based on the hysteretic behaviour of each wall panel in the time-domain, the local equivalent-linear panel properties are computed at each SSI iteration in the complex frequency-domain. The stiffness reduction is applied directly to the elastic modulus for each panel. This implies, under the isotropic material assumption, that the shear, axial and bending stiffness suffer the same level of degradation. Poisson ratio is considered to remain constant. Thus, in the current implementation, the wall panel shear stiffness modification as a result on nonlinear behaviour is fully coupled with the bending stiffness. This is a reasonable assumption only for the low-rise shearwalls for which the nonlinear behaviour is governed by the shear deformation. Based on various experimental tests done at the Cornell University, Gergely states in NUREG/CR 4123 (Gergely, 1984) that in low-rise walls such as those that occur in the modern nuclear power plants, the flexural distortions and associated vertical yielding play a negligible role. This was also recognized by other research studies, including the EPRI report on “Methodology for Developing Seismic Fragilities” (Reed and Kennedy, 1994).

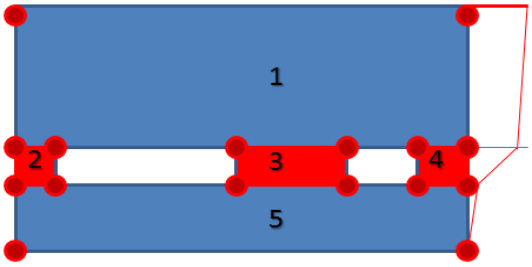

Figure 2 Panel Split Due to Openings

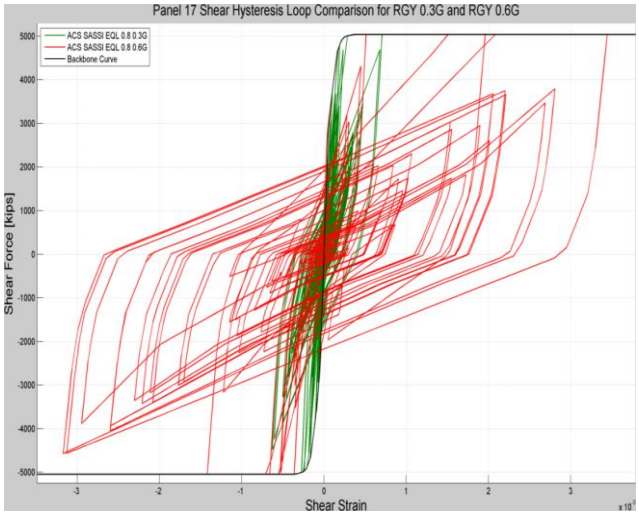

Figure 3 Hysteretic Loops for Two Strain Levels

The BBC for each panel depends on the panel geometry, thickness, concrete and reinforcement strengths and ratios. For each panel, analysts need to define the BBC curve. The BBC should be built based on the concrete cracking and ultimate wall capacities under either shear or bending deformation. The shear and bending strains in wall are determined based on the panel corner relative displacements after the rigid body transformation is subtracted. It should be noted that the horizontal and vertical displacements computed at the panel corners of each wall must include the combined effects of the three seismic component inputs.

The BBC curves should have a smooth shape and variation that describes the nonlinear behaviour of the wall panels under the lateral seismic loading. The BBC could be built based on the existing experimentally-based technical recommendations, or computed using static nonlinear pushover FE analysis. However, the BBC computed using pushover analysis could be quite different than experimentally-based BBC based on technical recommendations from different pertinent sources. This is an important aspect to be paid attention by the analyst. For estimating the low-rise shearwall panel capacities there are a significant number of pertinent sources in the literature that provide different empirical equations for computing the wall panel shear capacities (Gulec and Whittaker, 2009). Using the SHEAR command the user can check the computed shear capacity values based on different shear capacity equations. Using the BBCGEN command, smooth BBC curves can be automatically generated for many wall panels.

The SHEAR command calculates the peak shear strength of a single panel or all wall panels. The panel geometric data including the appropriate height, width and cross-sectional areas are automatically used by the SHEAR command for each panel. The SHEAR command uses four different peak shear equations, such as those provided by ACI 318-08, Wood, 1990, Barda et al., 1977 and Gulec-Whitakker, 2009 (Gulec and Whittaker, 2009). The lower bound value for Wood, 1990, and the upper bound value for Wood, 1990 and ACI 318-08 equations are also included. A total of six columns with computed peak shear strength are written for each panel. The columns of the result table are in the order of, the panel number, upper bound of ACI 318-08, ACI 318-08, Wood, 1990, lower bound of Wood, 1990, Barda, 1977 and Gulec-Whittaker, 2009. It should be noted that the popular Barda equation heavily used in the past for estimating the shear wall capacities, is basically applicable only to the barbell shear walls with heavy flanges, for other shear walls with small flanges Barda equation could significantly underestimate the shear capacities. Figure 4 shows a comparison of Barda, 1977 and Wood, 1990 equation results for the

same wall panel using the CMS hysteretic model. Recently, the Barda equation was taken out of the new ASCE 43-16 standard draft. Also, the Gulec-Whittaker equation is highly sensitive to the wall panel height/length ratios, so that for lower ratios, the shear capacities computed with this equation become unrealistically large.

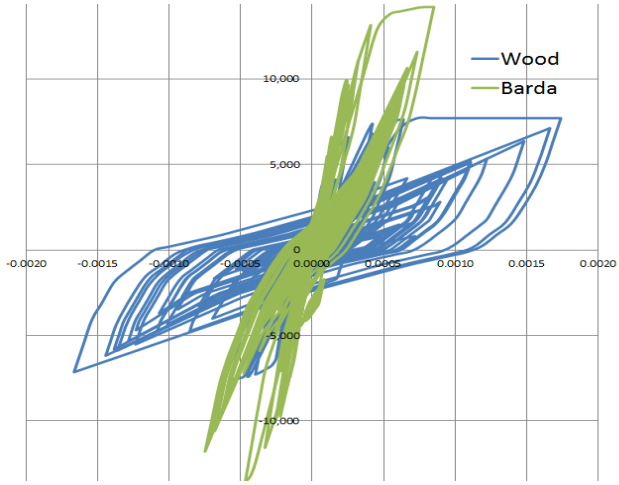

Figure 4 Barda, 1977 vs. Wood, 1990 Equation

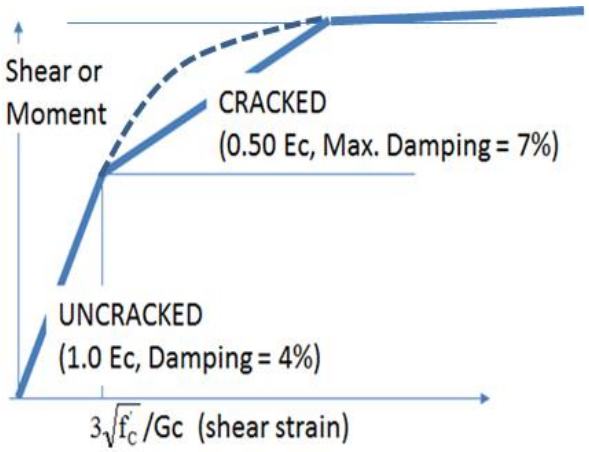

Figure 5 BBC Generation Using BBCGEN

The SHEAR command includes the following options for computing the wall panel shear capacities which are described by the equations shown below. In these equations, the F_{VW} force is the vertical reinforcement strength $F_{VW} = \rho_V A_W f_y$ (kips or kN), f'_c is the compressive strength (ksi or kN/m^2), fy is the reinforcement yield strength (ksi or kN/m^2), ρ_V or ρ_H, the web reinforcement ratio for the vertical direction or horizontal direction, Nu is axial force (kips or kN). The A_{BE} and F_{BE} parameters are used only in the Gulec-Whittaker equation. The Abe parameter defines the boundary element vertical reinforcement area (ft^2 or m^2) that is used to compute the boundary force $F_{BE} = A_{BE} f_{y,BE}$. The $f_{y,BE}$ parameter defines the boundary element vertical reinforcement yield stress (ksi or kN/m^2) that is used to compute the boundary force $F_{BE} = A_{BE} f_{y,BE}$.

Barda et al., 1977: The Barda equation (equation 2-7 or 4-7 in Gulec and Whittaker, 2009) is applicable to squat walls with heavily reinforced flanges (barbells). For typical shearwalls in nuclear facilities Barda equation could provide overly estimated shear strength values. Axial force effect is included.

$$V = \left(8\sqrt{f'_c} - 2.5\sqrt{f'_c}\,\frac{h_W}{l_W} + \frac{N_U}{4 l_W t_W} + \rho_V f_y \right) t_W (0.6 l_W) \qquad (1)$$

Wood, 1990: The Wood equation appears (equation 2-8 in Gulec and Whittaker, 2009) close to be quite close to the median estimates for ultimate shear strength for various squat wall tests. Axial force is not included.

$$6\sqrt{f'_c} A_W \le V = \frac{\rho_V A_W f_y}{4} \le 10\sqrt{f'_c} A_W \qquad (2)$$

ACI 318-08, 2008: The ACI 318-08 Chapter 11 equation appears (equation 4-1 in Gulec and Whittaker, 2009) could provide overly estimated ultimate shear strengths. Axial force is not included.

$$V = \left(\alpha_c \sqrt{f'_c} + \rho_H f_y\right) A_W \le 10\sqrt{f'_c} A_W \quad (3)$$

Gulec-Whittaker, 2009: The Gulec-Whittaker equation appears (equation 6-9 in Gulec and Whittaker, 2009) to be also close close to the median estimates for the ultimate shear strength for various squat wall tests. However, this Gulec-Whittaker equation is sensitive to the panel height/length aspect ratio. If this equation is applied to long panels the ultimate shear force goes up much closer to Barda, 1977 or ACI 318-08 shear force results, and even higher. Axial force is included.

$$V = \left(1.5\sqrt{f'_c} A_W + 0.25F_{VW} + 0.20F_{BE} + 0.40N_U\right) / \sqrt{h_W / l_W} \quad (4)$$

The BBCGEN command automatically generates BBC for a single panel, or for all panels using an ultimate wall shear capacity equation that is identical with one of the equations used by the SHEAR command, i.e. the equations 1-4 shown above.

Before using the BBCGEN command, the user needs to decide which of the four shear ultimate capacity models of the SHEAR command he would like to consider for the nonlinear SSI analysis. The shear capacity model can be also different for different wall panels. The smoothed BBC are automatically generated based on the input data on the cracking and ultimate shear force values and assuming that the secant cracked stiffness between the cracking and yielding points is half of the uncracked stiffness as recommended in the ASCE 4-16 and ASCE 43-5 standards, and USNRC SRP 3.7.2. The BBCGEN command also include to option for defining the cracking force: i) It defines the ratio between the cracking shear force and ultimate shear force to determine the cracking point of the BBC curve, i.e. this ratio varies between 0.10 and 0.50, and ii) It uses the ASCE 4-16 standard recommendation in Section C.3.3.2 for defining the cracking shear stress by $3\sqrt{f'_c}$. The BBC computed slopes at the ends of the interval between cracking and yielding points provide always smooth transitions independently of the user-selected option for defining cracking force as shown in Figure 5. The BBCGEN command always generates a 22 point BBC curves, the first point being the cracking point of the BBC curve. The next 20 points will be equidistantly spaced along the strain axis beyond the cracking point until the yield point is reached. The final shear failure point for all BBC curves will be defined by default at (shear strain = 2% and shear force = 1.02 x ultimate shear force value).

The ASCE 4-16 Section C3.3.2 recommends for the evaluation of the concrete cracking pattern for the site-specific applications, to use at the least a two-step procedure as described here. First, the linear SSI analysis is performed for the uncracked structure, to compute the stresses in structure walls. If the wall shear stress is larger than $3\sqrt{f'_c}$ (or shear strain larger than $3\sqrt{f'_c} / G_c$), or the wall bending stress is larger than $7.5\sqrt{f'_c}$ (or bending strain larger than $7.5\sqrt{f'_c} / E_c$), then, the concrete wall is considered fully cracked, so that its stiffness goes down to 50% of elastic stiffness, and its damping goes up to 7%. After, the concrete wall properties are changed accordingly in the structure model, the second SSI analysis is performed using the linearized partially cracked model to obtain the final SSI results. The ASCE 4-16 standard Section C3.3.2 states that *"After running the second analysis that includes cracked properties for some or all walls, rechecking the wall stress state is not necessary.*" In other words, the ASCE 4-16 standard considers that only 1 iteration linearized SSI analysis is reasonable accurate.

To be in full compliance with the ASCE 4-16 standard recommendations for the design-level analyses while running the ACS SASSI Option NON software, the analyst is required to define a cut-off damping value of 7%, so that computed material damping values for the concrete walls are not allowed to go higher than 7%. However, from a theoretical point of view, the nonlinear SSI analysis should be performed without any artificial damping cut and run SSI analysis iteratively until the convergence is fully reached. The convergence is achieved typically in about 2-4 SSI iterations for the design-level and about 4-8 SSI iterations for beyond design-level. The SSI iteration runtimes are typically 40-50% of the initial elastic SSI analysis runtime.

A comparison between the nonlinear SSI analysis results obtained using 7% cut-off damping value for concrete walls per the ASCE 4-16 recommendations and the nonlinear SSI solution with no damping cut-off is illustrated in next section.

EVALUATION OF CONCRETE CRACKING EFFECTS FOR A SHEARWALL BUILDING

A typical low-rise concrete shearwall nuclear building was considered (Figure 6). The seismic input at design-level was defined by a RG1.60 spectrum compatible acceleration history with 0.30g maximum amplitude. The soil deposit was idealized by a uniform rock formation with a shear wave velocity of 5,000 fps. The nonlinear structure model includes a total of 40 wall panels. The BBC for all walls are shown in Figure 7. The reinforced concrete wall nonlinear behaviour was idealized by the Cheng-Mertz (CMS) hysteretic model.

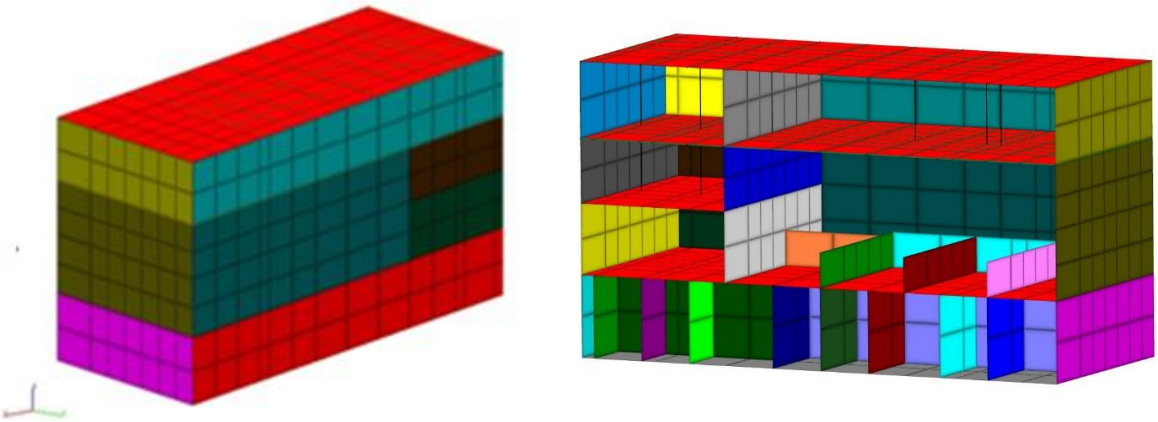

Figure 6 External and Internal Views of Shearwall Building Model Including 40 Nonlinear Wall Panels

Figure 8 indicates the selected SSI response locations of interest. These are two node locations, node 143 on the 4th floor (higher elevation) and node 570 on the 2nd floor (lower elevation), and the shear wall panel, Panel 17, that shows largest shear strains during earthquake duration.

Selected seismic SSI responses computed for the 0.30g RG1.60 design-level input are shown in Figures 9 thru 12. Figure 9 compares the linear elastic and the nonlinear SSI response normalized story drifts or shear strains for Panel 17. The computed maximum shear strain is about 0.02% for linear structure and about 0.5% for nonlinear structure. Thus, the nonlinear story drift is about 2.5 times larger for nonlinear structure than linear structure.

The effects of applying the conventional 7% cut-off damping value (blue line), as required by the ASCE standards and USNRC guidelines for the cracked concrete elements, on the structure hysteretic response is shown in Figure 10 for the Panel 17 story drift. It can be seen that the 7% damping cut-off effect increases the wall drift response by only 10% in comparison with the nonlinear fully converged solution with no damping cut-off. The nonlinear solutions are fully converged.

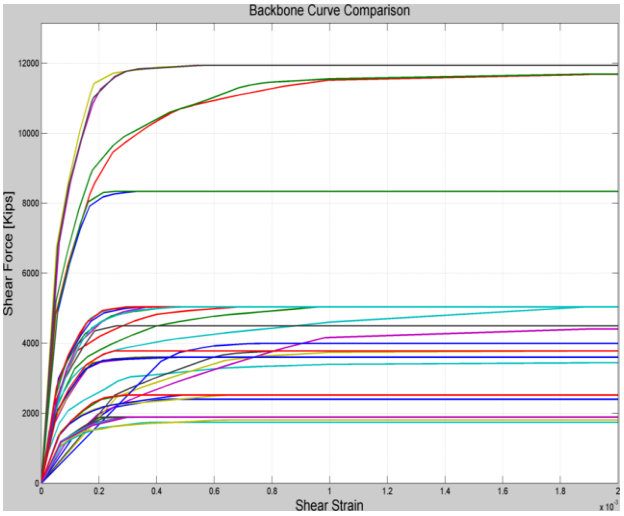

Figure 7 Computed BBC for Shearwall Panels

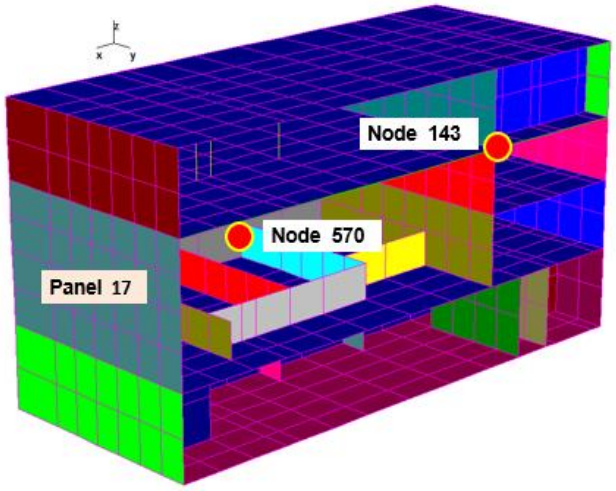

Figure 8 CMS Hysteretic Loops for 0.30g and 0.60g

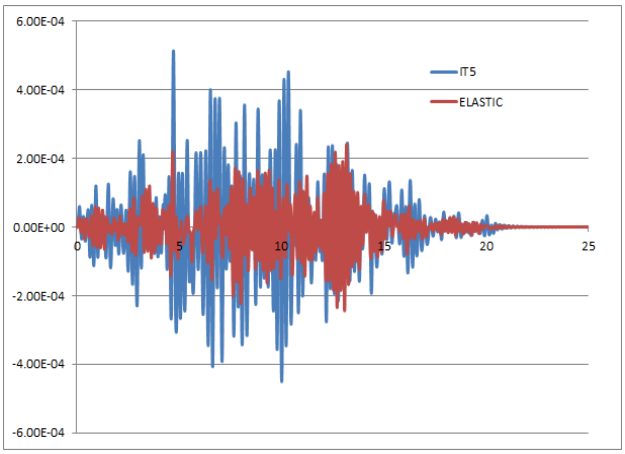

Figure 9 Panel 17 Linear and Nonlinear Strains

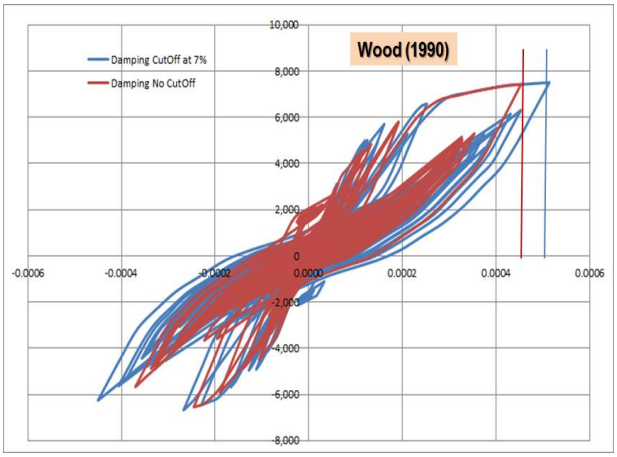

Figure 10 Hysteretic Effects of 7% Damping Cut-off

A comparison of the effective or iterated wall panel stiffness and damping values in all walls, with and without 7% damping cut-off is shown in Figure 11. The nonlinear SSI solution was fully converged. It should be again noted that the effect of introducing the conventional 7% damping cut-off as recommended by seismic design regulations has a very small impact on effective wall stiffness values, and more significant effect on the damping values. The main transverse walls are the Panels # 17, 19, 22-25 between 2nd and 4th floors (see Figure 1) which exhibit a significant concrete cracking, as their effective stiffness values drop to about 40%-65% of the initial uncracked concrete stiffness. These transverse walls have also larger hysteretic damping values greater than the 7%, up to 12% for the Panel 17 which is the most seismically loaded wall. It can be also observed that for the transverse walls between the 1st and 2nd floors the stiffness reduction is considerably less, not more than 15%-20%, since at this level there a large number of transverse walls.

Figure 12 shows the in-structure response spectra (ISRS) at lower and higher elevations in the structure. The two locations that correspond to the node 143 (higher elevation) and node 570 (lower elevation) are indicated in Figure 8. It should be noted that the effect of concrete cracking significantly affects the 5% damping ISRS results. The reduction of the ISRS peaks is about 40% for the higher elevation ISRS and

about 20% for the lower elevation ISRS. It should be also remarked that the nonlinear response ISRS computed without and with the 7% damping cut have very close values with differences of about 5% only. This shows again that the effect of introducing the artificial damping cut-off at 7% as required by the ASCE design codes is minimal.

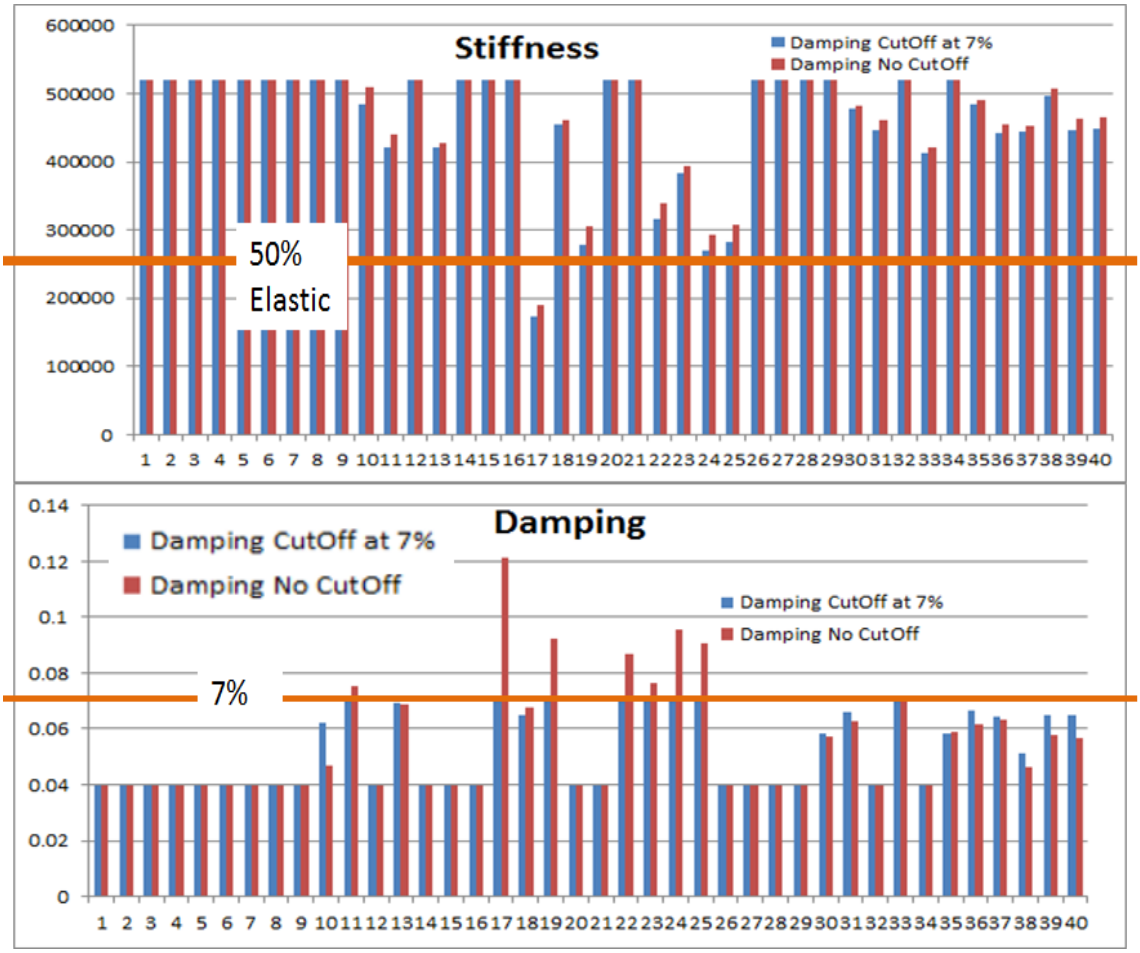

Figure 11 Effective Wall Stiffness and Damping Values for 0.30g Seismic Input

Figure 13 provides an additional insight related to the new ASCE 4-16 recommendations for considering concrete cracking for site-specific applications. This figure shows a comparison between the computed effective stiffness and damping values for the 7% damping cut-off SSI analysis based on a 1 iteration SSI analysis (It1) versus a fully converged 5 iteration SSI analysis (It5).

The computed effective wall stiffnesses of the transverse walls (Panels # 17, 19, 22-25) are 15%-25% smaller if the fully converged nonlinear solution is considered. These stiffness differences translate in 10%-12% differences in structural frequency as also indicated by the ISRS in Figure 12 for the higher elevation location. The comparative results in Figure 13 indicate that the 1 iteration SSI analysis simplified procedure recommended by the ASCE 4-16 standard appears to be reasonable for engineering response prediction purposes, especially that the 50% effective stiffness reduction in transverse walls is directly achieved based.

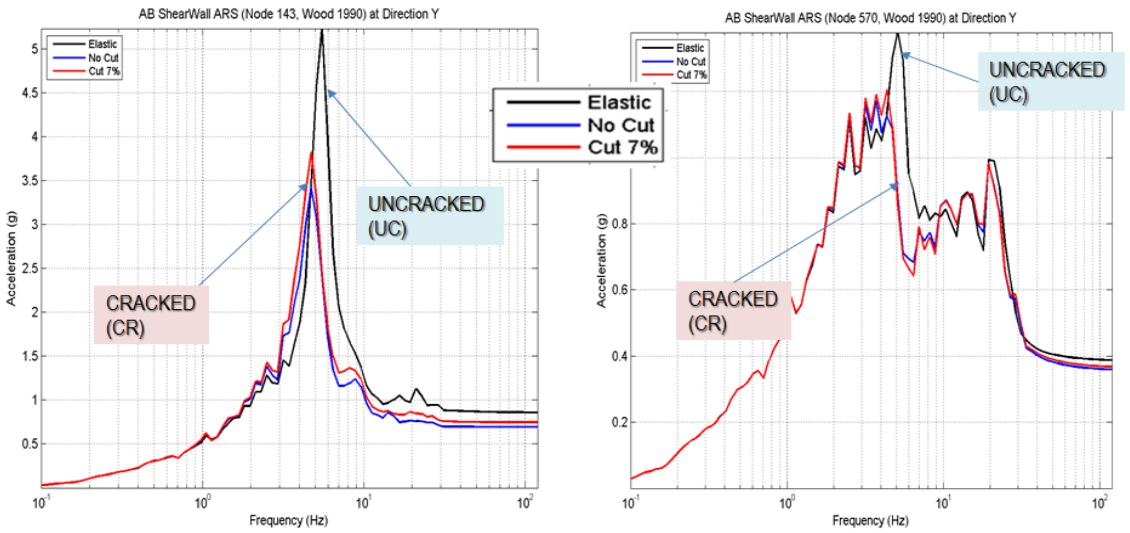

Figure 12 Effects of Damping Cut on the ISRS at Higher (Node 143) and Lower (Node 570) Elevations

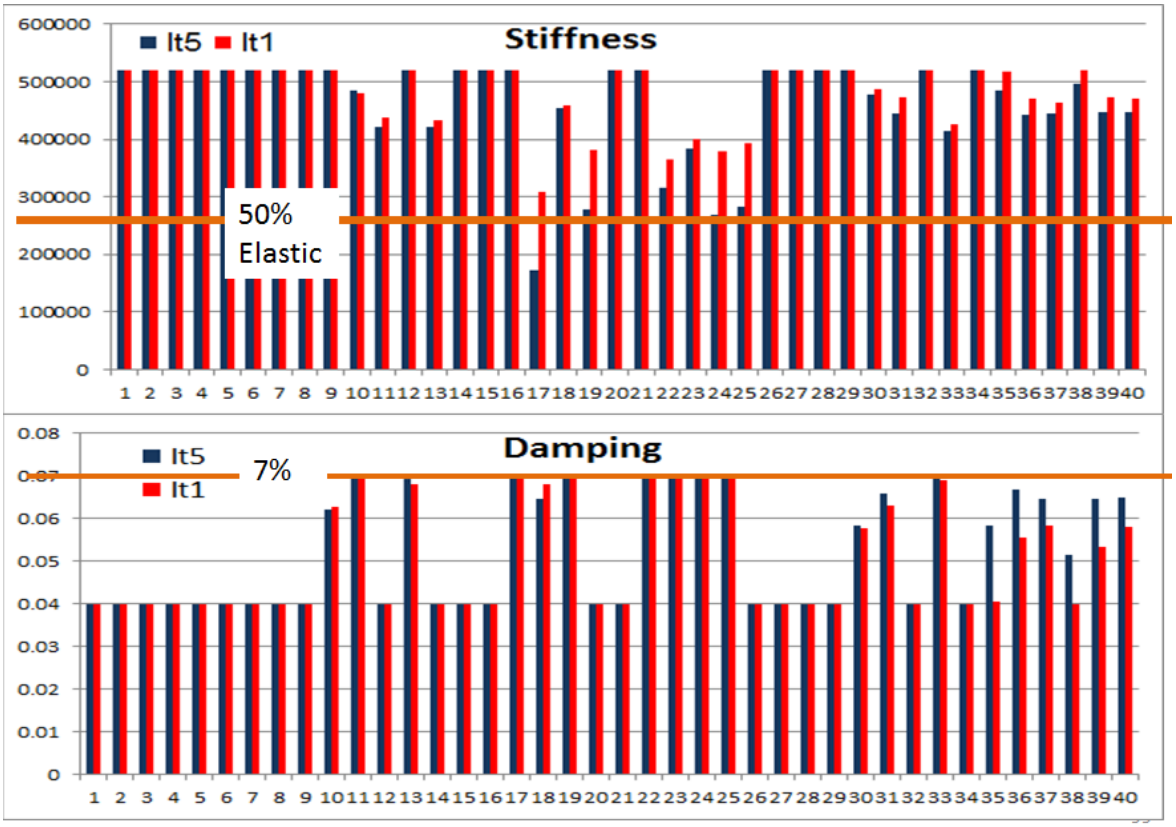

Figure 13 Effects of the Number of SSI Iterations for the 7% Cut-off Damping Case

An important nonlinear SSI modelling aspect to be carefully considered for nonlinear SSI modelling is the presence of openings within structural walls. Figure 14 shows the effects of an opening in an external wall on the building (about 1/3 of the wall length) for the design-level input. Due to the presence of the wall opening, the wall shear capacity goes down, while the shear strain goes up significantly. The existence of openings amplify the local stresses field surrounding the openings and by this creates pockets of "weak" nonlinear behaviour where the strains in concrete can be much larger than in other locations.

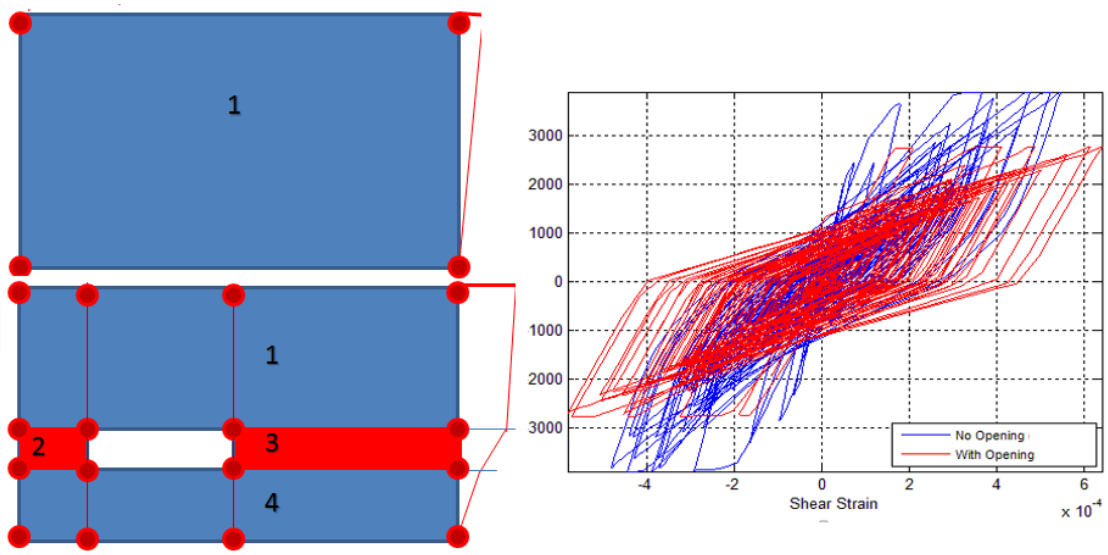

Figure 14 Effect of Large Opening on Wall Hysteretic Behaviour for 0.30g Design-Level Input

CONCLUSION

The paper shows the application of an efficient hybrid approach based on the iterative equivalent-linearization for performing a fast nonlinear SSI analysis to include the concrete wall cracking effects in accordance to the US practice requirements for the site-specific license applications. The paper compares the nonlinear SSI analysis results for a low-rise shearwall building with the results obtained using the same hybrid approach but limiting the equivalent-linear damping value in the concrete walls to 7%, as required by ASCE and USNRC regulatory documents. It is shown that the ASCE 4-16 Section C.3.3.2 requirements for performing SSI analysis for the partially cracked concrete models using the simple two-step procedure provides practical results for engineering practice purposes.

REFERENCES

American Society of Civil Engineers (2005) "Seismic Design Criteria for Structures, Systems, and Components in Nuclear Facilities", *ASCE 43-05 Standard.*

American Society of Civil Engineers (2017), "Seismic Analysis for Safety-related Nuclear Structures and Commentary" *ASCE 4-16 Standard*

Barda, F., J.M. Hanson, and G.W. Corley (1977) "Shear Strength of Low-Rise Walls with Boundary Elements", *ACI Special Publication SP 53-8.*

Cheng, Y.F. and Mertz, G. (1989)."Inelastic Seismic Response of Reinforced Concrete Low-Rise Shear Walls of Building Structures", *Univ. of Missouri-Rolla, Dept. of Civil Engineering,* CE 89-30

Gergely, P.(1984) "Seismic Fragility of Reinforced Concrete Structures and Components for Application in Nuclear Facilities", *Cornell University, Published as NUREG/CR-4123*

Ghiocel D.,M. (2015) "Fast Nonlinear Seismic SSI Analysis Using A Hybrid Time-Complex Frequency Approach For Low-Rise Nuclear Concrete Shearwall Buildings", *SMiRT22 Conference Proceedings,* Division V, Manchester, UK, August 10-14

Ghiocel Predictive Technologies, Inc. (2016). "ACS SASSI - An Advanced Computational Software for 3D Dynamic Analyses Including SSI Effects", ACS SASSI Version 3.0 Manuals, December 31,

Gulec, C.K. and A.S. Whittaker (2009). "Performance-Based Assessment and Design of Squat Reinforced Concrete Shear Walls", *Technical Report, MCEER, No. 09-0010*